Development and Application of a Deterministic Bank Stability and Toe Erosion Model for Stream Restoration

Andrew Simon

National Sedimentation Laboratory, Agricultural Research Service, USDA, Oxford, Mississippi, USA

Natasha Pollen-Bankhead and Robert E. Thomas[1]

National Sedimentation Laboratory, Agricultural Research Service, USDA, Oxford, Mississippi, USA

Department of Civil and Environmental Engineering, University of Tennessee, Knoxville, Tennessee, USA

The Bank Stability and Toe Erosion Model (BSTEM) is a spreadsheet tool used to simulate stream bank erosion in a mechanistic framework. It has been successfully used in a range of alluvial environments in both static mode to simulate bank stability conditions and design of stream bank stabilization measures and iteratively over a series of hydrographs to evaluate surficial, hydraulic erosion, bank failure frequency, and the volume of sediment eroded from a bank over a given time period. In combination with the submodel RipRoot, reinforcing effects of riparian vegetation can be quantified and included in analysis of mitigation strategies. The model is shown to be very useful in testing the effect of potential mitigation measures that might be used to reduce the frequency of bank instability and decrease sediment loadings from stream banks. Results of iterative BSTEM analysis are used to extrapolate volumes of bank-derived sediment from individual sites to reaches when used with observations of the "percent reach failing." Results show that contributions of suspended sediment from stream banks can vary considerably, ranging from 10% in the predominantly low-gradient, agricultural watershed of the Big Sioux River, South Dakota, to more than 50% in two steep, forested watersheds of the Lake Tahoe Basin, California. Modeling of stream bank mitigation strategies shows that toe protection added to eroding stream banks can reduce overall volumes of eroded sediment up to 85%–100%, notwithstanding, that hydraulic erosion of the toe in this case makes up only 15%–20% of total bank erosion. BSTEM is available to the public free of charge at http://www.ars.usda.gov/Research/docs.htm?docid=5044.

[1]Now at the School of Earth and Environment, University of Leeds, Leeds, UK.

Stream Restoration in Dynamic Fluvial Systems: Scientific Approaches, Analyses, and Tools
Geophysical Monograph Series 194

10.1029/2010GM001006

1. INTRODUCTION

Sediment is one of the leading contributors to water-quality impairment in surface waters of the United States through its adverse effects on water supply and aquatic life-support processes. Stream bank erosion by mass failure represents an important form of channel adjustment and a significant source of sediment in disturbed streams, often contributing 60%–80% of the suspended-sediment load [*Simon and Rinaldi*, 2006].

Given the relatively important role of stream bank erosion in watershed sediment yields and channel adjustment, it is surprising that little, if any, quantitative information is available on the effectiveness of bank treatments on reducing erosion. Further, mechanistic bank stability analyses are rarely conducted in restoration activities or sediment load estimates as part of restoration or erosion-control activities. Bank failures generally occur by a combination of hydraulic processes that undercut the base of the bank and geotechnical processes causing bank collapse by gravity. The variables and processes that control stream bank erosion need to be predicted accurately under existing and remediated conditions to evaluate bank stabilization designs, existing stream bank-derived sediment loads, and the potential to alter sediment loads from stream banks. The fundamental premise to reduce loadings from stream bank erosion is, therefore, to either reduce the hydraulic and downslope forces and/or to increase the resistance of the bank toe to hydraulic forces and the resistance of the bank mass to downslope (gravitational) forces. Mitigation measures to reduce bank erosion might include some combination of bank toe protection to increase resistance to hydraulic forces, planting of vegetation on the bank top and face to increase the cohesive strength of the bank materials thereby making them more resistant to mass failure, or regrading the bank slope to a flatter angle to reduce the overall driving downslope force. All of these processes and conditions can be simulated with the deterministic Bank Stability and Toe Erosion Model (BSTEM) [*Simon et al.*, 2000].

BSTEM has been used statically to test for relative stability of a bank under given pore water pressure and vegetation conditions [*Pollen and Simon*, 2005; *Pollen-Bankhead and Simon*, 2009], to test for stable bank slope designs [*Simon et al.*, 2008], and to determine the importance of seepage undercutting relative to bank strength, bank angle, pore water pressure, and root reinforcement [*Cancienne et al.*, 2008]. With time series pore water pressure data, the model has been used quasi-dynamically to evaluate the important variables controlling bank stability [*Simon et al.*, 2000] and the mechanical and hydrologic effects of riparian vegetation [*Simon and Collison*, 2002; *Simon et al.*, 2006]. Most recently, BSTEM has been used iteratively to simulate hydraulic erosion at the bank toe and bank stability during a series of flow events for the purpose of evaluating current (existing) and potential changes in failure frequency and stream bank-derived sediment loads [*Simon et al.*, 2010].

The purpose of this chapter is to demonstrate the application of BSTEM as a viable, mechanistic tool for three typical stream restoration objectives: (1) determining stable bank conditions under a variety of environmental conditions and erosion-control strategies, (2) quantifying bank-widening rates and sediment loads emanating from stream banks, and (3) determining potential reductions in widening rates and sediment loads under a range of mitigation techniques. The model is applied herein under static conditions to design a bank stabilization project and iteratively over a series of annual hydrographs in diverse environments to predict sediment loads and potential load reductions from stream bank erosion.

2. BANK STABILITY AND TOE EROSION MODEL

BSTEM is a mechanistic bank stability model specifically designed for alluvial channels. It is programmed in Visual Basic and exists in the Microsoft Excel environment as a simple spreadsheet tool. Data input, along with the various subroutines are included in different worksheets including Input Geometry, Bank Material, Bank Vegetation and Protection, Bank Model Output, and Toe Model Output. The user is able to move freely between worksheets according to their needs at various points of model application. BSTEM is available to the public free of charge at http://www.ars.usda.gov/Research/docs.htm?docid=5044.

2.1. General Model Capabilities

The original model developed by *Simon et al.* [1999, 2000] is a limit equilibrium analysis in which the Mohr-Coulomb failure criterion is used for the saturated part of the stream bank, and the *Fredlund et al.* [1978] criterion is used for the unsaturated part. The latter criterion indicates that apparent cohesion changes with matric suction (negative) pore water pressure, while effective cohesion remains constant. In addition to accounting for positive and negative pore water pressures, the model incorporates complex geometries, up to five user-definable layers, changes in soil unit weight based on water content, and external confining pressure from streamflow. Current versions combine three limit equilibrium-method models that calculate factor of safety (F_s) for multilayer stream banks. The methods simulated are horizontal layers [*Simon et al.*, 2000], vertical slices with tension crack [*Morgenstern and Price*, 1965], and cantilever failures [*Thorne and Tovey*, 1981]. The model can easily be adapted to incorporate the effects of geotextiles or other bank stabilization measures that affect soil strength.

The version of BSTEM used throughout this chapter (version 5) includes a submodel to predict bank toe and bank surface erosion and undercutting by hydraulic shear. This is based on an excess shear stress approach that is linked to the geotechnical algorithms. Complex geometries resulting from simulated bank toe erosion are used as the new input geometry for the geotechnical part of the bank stability model. The geometry of the potential failure plane can be input by the user or can be determined automatically by an iterative search routine that locates the most critical failure-plane geometry. If a failure is simulated, that new bank geometry can be exported back into either submodel to simulate conditions over time by running the submodels iteratively with different flow and water table conditions. In addition, the bank stability submodel automatically selects between cantilever and planar-failure modes. The mechanical, reinforcing effects of riparian vegetation [*Simon and Collison*, 2002; *Micheli and Kirchner*, 2002] can be included in model simulations. This is accomplished with the RipRoot model [*Pollen and Simon*, 2005] that is based on fiber-bundle theory and included in the Bank Vegetation and Protection worksheet. The current version of BSTEM (version 5) also includes new features that can account for enhanced hydraulic stresses on the outside of meander bends as well as reduced, effective hydraulic stress operating on fine-grained materials in a reach characterized by a rougher boundary.

2.1.1. Bank-Toe Erosion Submodel. The Bank-Toe Erosion submodel is used to estimate erosion of bank and bank toe materials by hydraulic shear stresses. The effects of toe protection are incorporated into the analysis by changing the characteristics of the toe material in the model. The model calculates an average boundary shear stress from channel geometry and flow parameters using a rectangular-shaped hydrograph defined by flow depth and the duration of the flow (steady, uniform flow). The assumption of steady, uniform flow is not critical insomuch as the model does not attempt to rout flow and sediment and is used only to establish the boundary shear stress for a specified duration along the bank surface. The model also allows for different critical shear stress and erodibility of separate zones with potentially different materials at the bank and bank toe. The bed elevation is fixed because the model does not incorporate the simulation of bed sediment transport. Toe erosion by hydraulic shear is calculated using an excess shear approach. The average boundary shear stress (τ_o) acting on each node of the bank material is calculated using

$$\tau_o = \gamma_w RS, \tag{1}$$

where τ_o is average boundary shear stress (Pa), γ_w is unit weight of water (9.81 kN m^{-3}), R is local hydraulic radius (m), and S is channel slope (m m^{-1}).

The average boundary shear stress exerted by the flow on each node of the bank profile is determined by dividing the flow area at a cross section into segments. A line is generated that separates the bed- and bank-affected segments (starting at the base of the bank and extending to the water surface) at an angle equal to the average of the bank and bank toe angles. The hydraulic radius (R) of the flow on each segment is the area of the segment (A) divided by the wetted perimeter of the segment (P_n). Thus, the shear stress varies along the bank surface according to equation (1) as parameters comprising the segmented areas change.

An average erosion rate (in m s^{-1}) is computed for each node by utilizing an excess shear stress approach [*Partheniades*, 1965]. This rate is then integrated with respect to time to yield an average erosion distance in centimeters. This method is similar to that employed in the CONCEPTS model [*Langendoen*, 2000], except that here, erosion is simulated to occur normal to the local bank angle and not horizontally:

$$E = k \quad \Delta t(\tau_o - \tau_c), \tag{2}$$

where E is erosion distance (cm), k is erodibility coefficient (cm^3 (N-s)$^{-1}$), Δt is time step (s), τ_o is average boundary shear stress (Pa), and τ_c is critical shear stress (Pa).

Resistance of bank toe and bank surface materials to erosion by hydraulic shear is handled differently for cohesive and noncohesive materials. Originally, for cohesive materials, the relation developed by *Hanson and Simon* [2001] using a submerged jet test device [*Hanson*, 1990, 1991] was used

$$k = 0.2\tau_c^{-0.5}. \tag{3a}$$

This relation has been recently updated based on hundreds of tests on stream banks across the United Sates [*Simon et al.*, this volume]:

$$k = 1.62\tau_c^{-0.838}. \tag{3b}$$

The *Shields* [1936] criterion is used for resistance of noncohesive materials as a function of roughness and particle size (weight) and is expressed in terms of a dimensionless critical shear stress:

$$\tau_c^* = \tau_o/[(\rho_s - \rho_w)gD], \tag{4}$$

where τ_c* is critical dimensionless shear stress, ρ_s is sediment density (kg m^{-3}), ρ_w is water density (kg m^{-3}), g is gravitational acceleration (m s^{-2}), and D is characteristic particle diameter (m).

2.1.2. Bank Stability Submodel. The bank stability submodel combines three limit equilibrium methods to calculate a factor of safety (F_s) for multilayered stream banks. The methods simulated are horizontal layers [*Simon and Curini*, 1998; *Simon et al.*, 2000], vertical slices for failures with a tension crack [*Morgenstern and Price*, 1965], and cantilever failures [*Thorne and Tovey*, 1981].

For planar failures without a tension crack, the factor of safety (F_s) for both the saturated and unsaturated parts of the failure plane is given by the ratio of the resisting and driving forces:

$$F_s = \frac{\sum_{i=1}^{I} (c_i' L_i + S_i \tan \phi_i^b + [W_i \cos \beta - U_i + P_i \cos (\alpha - \beta)] \tan \phi_i')}{\sum_{i=1}^{I} (W_i \sin \beta - P_i \sin [\alpha - \beta])}, \tag{5}$$

where c_i' is effective cohesion of ith layer (kPa), L_i is length of the failure plane incorporated within the ith layer (m), S_i is force produced by matric suction on the unsaturated part of the failure surface (kN m^{-1}), ϕ^b is angle representing the rate of increase in shear strength with increasing matric suction (degrees), W_i is weight of the ith layer (kN), U_i is the hydrostatic-uplift force on the saturated portion of the failure surface (kN m^{-1}), P_i is the hydrostatic-confining force due to external water level (kN m^{-1}), β is failure-plane angle (degrees from horizontal), α is bank angle (degrees from horizontal), ϕ' is angle of internal friction (degrees), and I is the number of layers.

The cantilever shear failure algorithm is a further development of the method employed in the CONCEPTS model [*Langendoen*, 2000]. BSTEM can utilize the different failure algorithms depending on the geometry and conditions of the bank. Determining whether a failure is planar or cantilever is based on whether there is undercutting and then comparing the factor of safety values. The failure mode is automatically determined by the smaller of the two values. The model is easily adapted to incorporate the effects of geotextiles or other bank stabilization measures that affect soil strength. This current version (5) of the model assumes hydrostatic conditions below the water table. Matric suction above the water table (negative pore water pressure) is calculated by linear extrapolation.

2.1.3. Root Reinforcement (RipRoot) Submodel. Waldron [1977] extended the Coulomb equation for root-permeated soils by assuming that all roots extended vertically across a horizontal shearing zone and that the roots act like laterally loaded piles, with tension transferred to them as the soil is sheared. In the *Waldron* [1977] model, the tension developed in the root as the soil is sheared is resolved into a tangential component resisting shear and a normal component increasing the confining pressure on the shear plane. ΔS can be represented by

$$\Delta S = T_r(\sin \theta + \cos \theta \tan \phi)(A_R/A), \tag{6}$$

where T_r is the average tensile strength of roots per unit area of soil (kPa), A_R/A is the root area ratio (dimensionless), and θ is the angle of shear distortion in the shear zone.

Gray [1974] reported that the angle of internal friction of the soil appeared to be affected little by the presence of roots. Sensitivity analyses carried out by *Wu et al.* [1979] showed that the value of the first angle term in equation (6) is fairly insensitive to normal variations in θ and ϕ (40°–90° and 25°–40°, respectively) with values ranging from 1.0 to 1.3. A value of 1.2 was therefore selected by *Wu et al.* [1979] to replace the angle term, and the simplified equation becomes

$$\Delta S = 1.2 T_r (A_R/A). \tag{7}$$

According to the simple perpendicular root model of *Wu et al.* [1979], the magnitude of reinforcement simply depends on the amount and strength of roots present in the soil. However, *Pollen et al.* [2004] and *Pollen and Simon* [2005] found that these perpendicular root models tend to overestimate root reinforcement due to the inherent assumption that the full tensile strength of each root is mobilized during soil shearing and that the roots all break simultaneously. This overestimation was largely corrected by *Pollen and Simon* [2005] by constructing a fiber-bundle model (RipRoot) to account for progressive breaking during mass failure. Validation of RipRoot versus the perpendicular model of *Wu et al.* [1979] was carried out by comparing results of root-permeated and nonroot-permeated direct-shear tests. The direct-shear tests revealed that accuracy was improved by an order of magnitude by using RipRoot estimates [*Pollen and Simon*, 2005; *Mickovski et al.*, 2009].

A later paper by *Pollen* [2007] investigated the forces required to pull out roots in a field study, and the RipRoot model was modified to account for both root failure mechanisms. The addition of pullout forces allowed for estimations of spatial variability in root reinforcement with changes in soil texture and temporal changes with changes in soil water. In the RipRoot model currently embedded in BSTEM 5, a vegetation assemblage can be created by accessing the species database contained in the submodel; the user enters species, approximate vegetation ages, and approximate percent cover of each species at each site to estimate root density. This database includes tests performed across the United States. Root reinforcement values are then calculated automatically using RipRoot's progressive breaking algorithm.

Table 1. Required User-Input Parameters for BSTEM[a]

Driving Forces			Resisting Forces		
Parameter	Purpose	Source	Parameter	Purpose	Source
Hydraulic Processes: Bank Surface					
Channel slope (S)	boundary shear stress (τ_o)	field survey or design plan	particle diameter (D) (cohesionless)	critical shear stress (τ_c)	bulk sample particle size (cohesionless); default values in model
			critical shear stress (τ_c) (cohesive)	critical shear stress (τ_c)	jet test (cohesive); default values in model
Flow depth (h)	boundary shear stress (τ_o)	field survey, gauge information, design plan	particle diameter (D) (cohesionless)	erodibility coefficient (k)	bulk sample particle size (cohesionless); default values in model
			critical shear stress (τ_c) (cohesive)	erodibility coefficient (k)	jet test (cohesive); default values in model
Unit weight of water (γ_w)	boundary shear stress (τ_o)	considered constant, 9810 N m^{-3}			
Geotechnical Processes: Bank Mass					
Unit weight of sediment (γ_s)	Weight (W), Normal force (σ)	core sample in bank unit; default values in model	unit weight of sediment (γ_s)	weight (W), normal force (σ)	core sample in bank unit; default values in model
Bank height (H)	Shear stress	field survey or design plan	effective cohesion (c')	shear strength (τ_f)	borehole shear, direct shear, triaxial shear; default values in model
Bank angle (α)	Shear stress	field survey or design plan	effective friction angle (ϕ')	shear strength (τ_f)	
			pore water pressure (μ_w)	shear strength (τ_f)	interpolated from water table

[a]Default values for geotechnical parameters are shown in Table 2.

2.2. Data Requirements

As BSTEM is a mechanistic model, the data required to operate the model are all related to quantifying the driving and resisting forces that control the hydraulic and geotechnical processes that operate on a stream bank. Input-parameter values can all be obtained directly from field surveying and testing. If this is not possible, the model provides default values by material type for many parameters. It has been our experience that all of the data needed to run BSTEM can be collected at a site by a crew of four within 1 day. Required data fall into three broad categories: (1) bank geometry and stratigraphy, (2) hydraulic data, and (3) geotechnical data. A summary of the required input parameters is provided in Table 1. The default geotechnical values that are included in the model are provided in Table 2.

2.3. General Model Limitations

BSTEM can simulate the most common types of bank failures that typically occur along alluvial channels. Once failure is simulated, the failed material is assumed to enter the flow. The model does not simulate rotational failures that generally occur in very high banks of homogeneous, fine-grained materials characterized by low bank angles. Although potentially damaging with regard to the amount of

Table 2. Default Values in BSTEM for Geotechnical Properties[a]

Soil Type	Statistic	c' (kPa)	ϕ' (°)	γ_{sat}(kN m^{-3})
Gravel (uniform)[b]		**0.0**	**36.0**	**20.0**
Sand and gravel[b]		**0.0**	**47.0**	**21.0**
Sand	75th percentile	1.0	32.3	19.1
	median	**0.4**	**30.3**	**18.5**
	25th percentile	0.0	25.7	17.9
Loam	75th percentile	8.3	29.9	19.2
	median	**4.3**	**26.6**	**18.0**
	25th percentile	2.2	16.7	17.4
Clay	75th percentile	12.6	26.4	18.3
	median	**8.2**	**21.1**	**17.7**
	25th percentile	3.7	11.4	16.9

[a]Data derived from more than 800 in situ direct-shear tests with the Iowa Borehole Shear Tester except where indicated. BSTEM values are indicated in bold.
[b]Data from *Hoek and Bray* [1977].

Table 3. Potential Alternative Means to Control the Two Primary Processes That Control Stream Bank Stability

Means of Control	Hydraulic Protection	Geotechnical Protection
Increase critical shear stress	bank toe and face armoring with rock, large wood, live vegetation	
Decrease applied shear stress	redirect flows, reduce channel slope (remeandering), increase bottom width, live vegetation (increased roughness)	
Increase bank shear strength		pole and post plantings, bank top vegetation, brush layers, drainage
Decrease driving, gravitational forces		reduce bank height, terraces, flatten bank slope; buttress bank toe

land loss, these failures are not common along alluvial streams. Another limitation of the current version of BSTEM is that it cannot simulate a dynamic water table and, therefore, dynamic pore water pressure distributions. The elevation of the phreatic surface must be input by the user. Vertical distributions of pore water pressure (below the water table) and matric suction (above the water table) are then calculated by the model through linear interpolation. Bank undercutting by seepage erosion is similarly not included in the version described herein. Finally, the hydrologic effects of riparian vegetation, including interception, evapotranspiration, and the accelerated delivery of water along roots and macropores cannot be simulated at this time. A research version of BSTEM currently used by scientists at the U.S. Department of Agriculture Agricultural Research Service National Sedimentation Laboratory does include a near-bank groundwater submodel that permits dynamic adjustment of pore water pressures over extended hydrographs. This dynamic version of BSTEM will be made available to the public in the near future.

3. BANK STABILITY MODELING FOR STREAM RESTORATION

Bank stability modeling is an important, if not critical, component of stream restoration or erosion-control activities that pertain to excess sediment loads or potential risk of adjacent lands and infrastructure. There are at least three restoration objectives that can benefit greatly from the use of a mechanistic tool to reliably predict sediment loadings and widening rates from stream bank erosion. These include the following: (1) determining bank stability conditions under a range of hydraulic and geotechnical conditions and erosion-control strategies, which includes designing sustainable bank stabilization measures and determining unstable bank conditions to assure continued delivery of sediment to the channel (in cases where there is insufficient supply [i.e., *Wyżga et al.*, this volume]), (2) quantifying bank-widening rates and sediment loads emanating from stream banks, and (3) determining potential reductions in widening rates and sediment loads under a range of mitigation techniques.

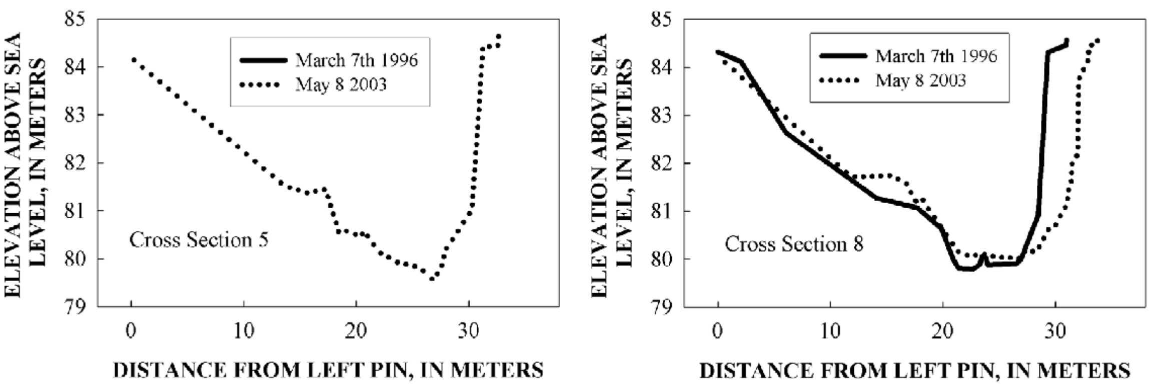

Figure 1. Changes in geometry between March 1996 and May 2003 at two cross sections along the Goodwin Creek bendway showing continued bank retreat. Modified from the work of *Simon et al.* [2008], reprinted with permission from American Society of Civil Engineers (ASCE).

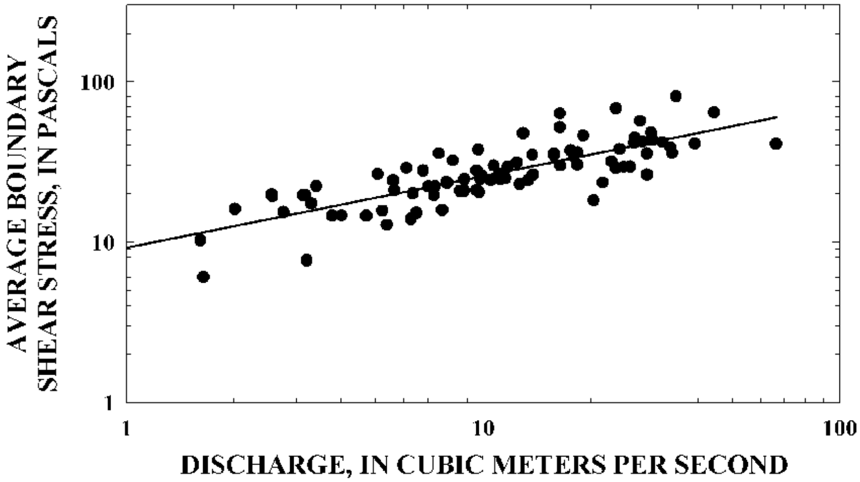

Figure 2. Relation between discharge and average boundary shear stress (τ_o) in the Goodwin Creek bendway. Data are calculated by multiplying measured peak flow depths with bed slope and unit weight of water.

Any restoration objective that requires reduction of sediment loads from stream banks must focus on mitigation measures that directly affect the processes that control stream bank stability, namely, hydraulic erosion and geotechnical instability (Table 3). Protection from hydraulic processes must either reduce the available boundary shear stress and/or increase the shear resistance to particle detachment, thereby reducing the likelihood and magnitude of bank toe steepening. Protection from geotechnical instability must focus on increasing soil shear strength and/or decreasing the driving (gravitational) forces to reduce the likelihood of mass failure of the upper bank.

Implementation of any design plan requires the analysis of the hydraulic and geotechnical processes likely to exist at the site, particularly during worst-case conditions. For hydraulic processes, these occur at peak flows when boundary shear stresses are greatest. For geotechnical processes, these generally occur during a wet period and following recession of peak stage when pore water pressures in the bank are at a maximum, and the confining pressure provided by the flow on the bank has been lost. This is referred to as the "draw-down" condition.

To address the first objective (above), BSTEM can be run for worst-case conditions under existing conditions to test

Table 4. Data Requirements for Using Riprap Sizing Spreadsheet[a]

Parameter (Symbol)	Units	Comments/Values
Channel width (W)	m	from field survey or design plan
Flow depth (h)	m	worst-case design flow or gauge information
Bed slope (S)	m m^{-1}	from field survey or design plan
Bank angle (θ)	degrees	from field survey or design plan
Specific gravity (G)	dimensionless	considered constant: 2.65
Angle of repose of rip rap (ϕ)	degrees	from literature[b]
Critical Shields parameter (τ^*_c)	dimensionless	typical: 0.032, 0.047, 0.06
Specific weight of water (γ_w)	N m^{-3}	considered constant: 9810 N m^{-3}

[a]Data requirements are by *Julien* [2002].

[b]See the work of *Simons and Sentruk* [1992, p. 413] and/or the work of *Selby* [1982, p. 54].

Table 5. Riprap Sizing Results Using *Julien*'s [2002] Spreadsheet Tool[a]

Flow Depth (m)	Slope	τ_c*	Size (cm)
3	0.003	0.032	*38.0*
3.5	0.003	0.032	*44.3*
4	0.003	0.032	*50.6*
4.5	0.003	0.032	*56.9*
3	0.003	0.047	25.9
3.5	0.003	0.047	30.2
4	0.003	0.047	34.5
4.5	0.003	0.047	38.8
3	0.003	0.06	20.3
3.5	0.003	0.06	23.6
4	0.003	0.06	27.0
4.5	0.003	0.06	30.4

[a]Implementation was based on the most conservative results (in italics); maximum stone sizes calculated at τ_c* of 0.032.

Table 6. Measured Geotechnical Parameters Used in Bank Stability Modeling

Layer	Friction Angle (deg)	Effective Cohesion (kPa)	Saturated Unit Weight (kN m^{-3})
1	33.1	1.4	16.9
2	28.1	2.7	19.3
3	28.1	2.7	19.3
4	27.0	6.3	20.0
5	36.0	0.0	20.0

whether "no action" is a viable option. Perhaps a single failure episode which will result in a flatter bank angle may be sufficient to reduce widening rates and sediment loads. If this is not the case, BSTEM can be run testing various combinations of mitigation strategies (Table 3) again under worst-case conditions. Restoration activities that involve one of the other two objectives (above) need to rely on iterative simulations with BSTEM over some specified period. This may be an annual hydrograph, series of annual hydrographs, or a selection of annual hydrographs representing the range of the annual flow series. Results from this latter approach can then use weighted load values (based on frequency of occurrence) to obtain mean annual loading rates. The following case studies will provide example applications for each of these restoration objectives.

3.1. Restoration Objective 1: Designing a Sustainable Bank Stabilization Project

Periodic channel surveys of a 4.7 m high bendway on Goodwin Creek, Mississippi, United States, during the period 1977 to 1996, in conjunction with dating of woody vegetation growing on the channel banks and bars at the study site, disclosed that rates of bank failure and channel migration over the period were relatively uniform at about 0.5 m yr^{-1}. Surveys conducted after every major flow event between 1996 and 2007 showed that migration rates continued at about 0.5 m yr^{-1}, resulting in about 20 m of bank retreat between 1966 and 2006 and the types of channel changes shown in Figure 1.

Based on fundamental processes of stream bank stability and knowledge attained from field observations, it was apparent that both hydraulic and geotechnical protection would probably be required to stabilize the 100 m long reach (Table 3). Hydraulically, the concept was to provide greater roughness and erosion resistance to the bank toe region. Bank toe protection was to be conducted using rock for two primary reasons. First, the use of engineered log jams in deeply incised streams of the southeastern United States has not been successful in some cases [*Shields*, 2003; *Shields et al.*, 2004]. Second, the cooperator on the project from the U. S. Army Corps of Engineers had great experience and success with using rock at the bank toe to resist hydraulic erosion and undercutting. Options for the design of the upper part of the bank were limited due to landowner constraints requiring the plan to retain a field road whose edge was located 5 m from the bank top edge. Thus, if required, bank slopes could only be flattened from the preproject slope of 75°–80° to 45° (1:1). Because the top bank edge could only be moved about 2 m landward, construction of the 1:1 slope would have to take place by filling, using material derived from the point bar on the inside part of the bend. In addition, if additional bank material strength was required to increase the shearing resistance of the bank mass, a planting scheme was devised using a range of woody riparian species to provide root reinforcement.

Stone size was selected based on a simple one-dimensional hydraulic analysis [*Julien*, 2002] such that the stone would not be mobilized at peak flows where average boundary shear stresses can reach 60–80 N m^{-2} (Pa) (Figure 2). Data required for this analysis can be obtained in the field or, for

Table 7. Summary of Simulation Results Using BSTEM for Goodwin Creek Bendway Representing Existing, After Initial Bank Failure, and Designed 1:1 Slope Geometries for the Case of Low-Flow and Drawdown Conditions[a]

Case	Geometry	Dominant Vegetation	Groundwater Elevation	F_s	Interpretation
1	existing	none	at flow level	1.10–1.56	stable
2	existing	none	moderate	0.87	unstable
3	after failure	none	moderate	1.44	stable
4	after failure	none	high	0.45	unstable
5	1:1 slope	none	moderate	2.10	stable
6	1:1 slope	none	high	0.67	unstable
7	1:1 slope	black willow	high	0.81	unstable
8	**1:1 slope**	**eastern sycamore, river birch**	**high**	**1.28**	**stable**

[a]Case 8 (bold) represents most stable design case.

Figure 3. View of the bendway looking upstream (left) from January 2006 and immediately following construction in March 2007. (middle) Note edge of constructed rock riffle in lower right and (right) stone-toe protection with three bendway weirs. From the work of *Simon et al.* [2008], reprinted with permission from ASCE.

the case of angle of repose for rip rap, from literature values [*Simons and Sentruk*, 1992, p. 413; *Selby*, 1982, p. 54] (see Table 4). Calculations were made for 3.0 to 4.5 m deep flows at a slope of 0.003 using typical Shields parameter values (τ_c*) of 0.032, 0.047, and 0.06 (Table 5). The most conservative results were obtained using the lowest value of τ_c* (0.032). Results for this case showed recommended stone sizes of 38 cm for the 3 m deep flow to 57 cm for the 4.5 m deep flow. From this analysis, it was determined that a combination of R-200 and R-650 stone, graded from 2.5 to 40 and 60 cm, respectively, would be sufficient.

Geotechnical data on bank material shear strength were collected during earlier phases of the bendway research (see Table 6); BSTEM version 5 was employed to simulate stability for preconstruction and initial (1:1 slope) design conditions. Effective cohesion and friction angle were obtained in situ using a borehole shear test device [*Lohnes and Handy*, 1968; *Lutenegger and Hallberg*, 1981]. Simulation of existing bank stability conditions supported observations over the past 10 years where, under low-flow conditions and a relatively deep near-bank groundwater table, banks were stable but become unstable with higher levels of saturation (Table 7). Keeping the geotechnical properties of the banks constant, the simulations were repeated with the designed 1:1 geometry. Much like the results for the existing geometry, the designed slope would be stable at low-flow conditions but unstable for the drawdown case (Table 7). In an attempt to increase the factor of safety under drawdown conditions, simulations were conducted to include root reinforcement provided by common riparian species in the top 1.0 m of the bank [*Simon and Collison*, 2002; *Pollen and Simon*, 2005]. This was attempted initially using black willow because this is one of the most commonly used woody riparian species in restoration work. Results, however, produced a F_s of 0.81, still indicative of instability. Simulations were repeated with eastern sycamore, which has been shown along with river birch to provide the greatest amount of root reinforcement over the top 1.0 m of the bank [*Simon and Collison*, 2002]. In this case, the F_s for the critical, drawdown case increased to 1.28, at the upper limit

Figure 4. Views of the Goodwin Creek bendway looking downstream during (left) February 1997 (pre project) and (right) July 2009 (post project). Construction took place 26 February to 2 March 2007.

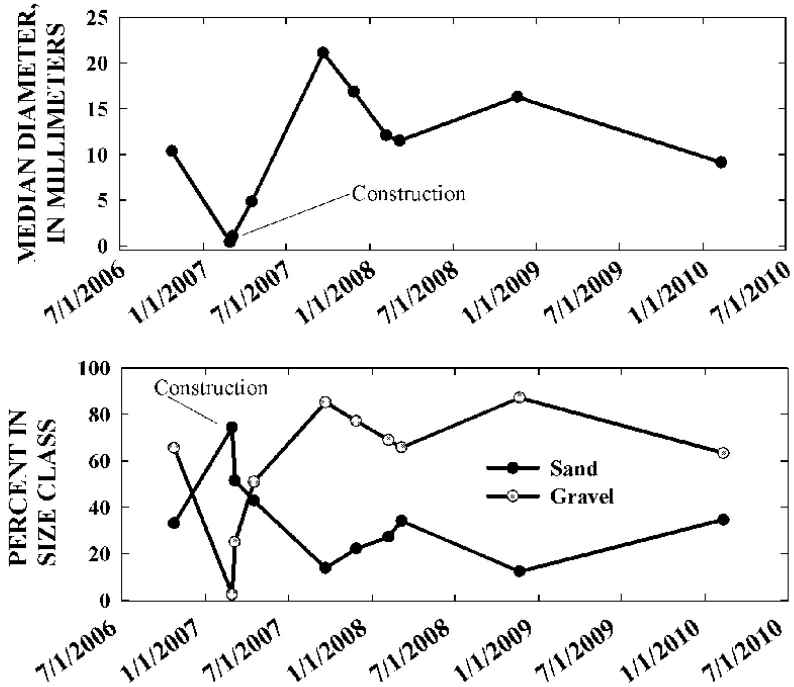

Figure 5. Variation in bed material particle size. Note the shift to sand bed during construction and the return to gravel bed following flushing of the fine material following construction.

of conditional stability. It is important to note, however, that it may take up to 3 years for riparian plants to start providing significant root reinforcement to the bank.

3.1.1. Final Design and Implementation. Based on the hydraulic and geotechnical analysis described in the preceding section, the overall design plan was implemented. About 275 t of both R-200 and R-650 stone costing between \$27 t^{-1} and \$33 t^{-1} were delivered to the site in late February 2007. Stone-toe protection along with three bendway weirs were constructed and placed. Material from the point bar was excavated and used to build the 1:1 slope on the left bank. All woody material removed from the bar was reused on the constructed bank. Vegetation that was excavated whole was

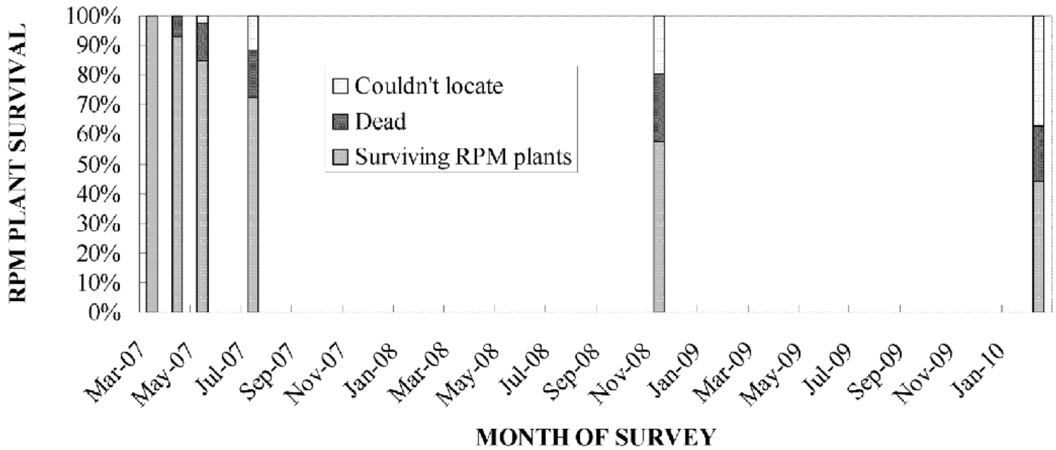

Figure 6. Survival rate of purchased root production method (RPM) plants between construction (March 2007) and February 2010. Note RPM indicates root production method, which produces faster growth and greater root biomass.

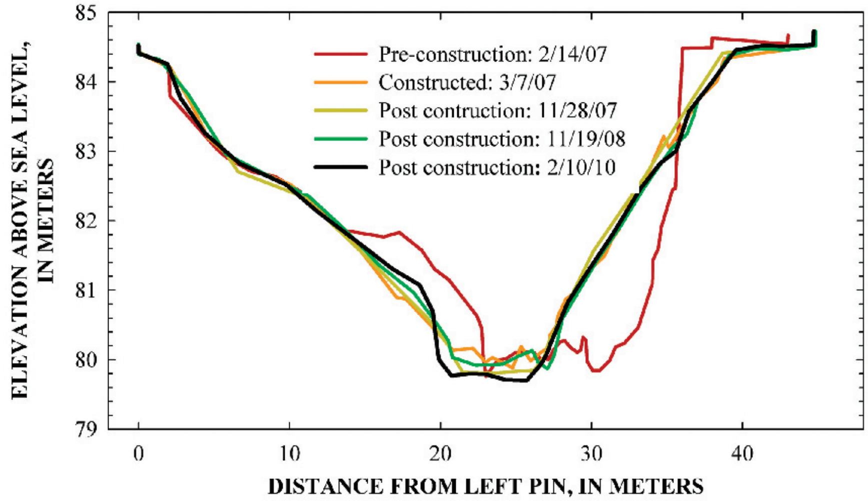

Plate 1. Comparison of channel geometry at cross section 8 (see Figure 1). Differences in bank geometry are largely a function of rod placement during surveys. Note streambed scour between March and November 2007. Dashed line represents highest stage over the period.

replanted on the constructed bank (including mature trees). Native species were selected and purchased based on the dominant species of surrounding riparian buffers, with assemblages largely composed of sycamore, river birch, and sweetgum trees. Other vegetation was cut and trimmed with the branches used for post plantings, and stems were placed on the ground along the contour to intercept overland flow that might be generated from the field road. The entire bank was then seeded with grass and overlain with straw (Figure 3). Construction took place between 26 February and 2 March. The cost of the entire project was $33,000 or $330 m^{-1}.

3.1.2. Postproject Monitoring. To evaluate the performance of the design scheme, a limited monitoring program was put in place following construction. Immediately following construction, the reach was surveyed, and samples of bed material were taken at numerous cross sections. Each of the purchased plants was tagged, their diameter was noted, and they were located with a GPS unit. Discharge was monitored continuously at the stream gauges just upstream of the reach.

Over the period March 2007 to February 2010, there was no hydraulic erosion at the bank toe and no mass failures of the upper part of the bank (Figure 4). The most significant change in the channel was up to 0.5 m of scour along some parts of the streambed (Plate 1). This was expected because of (1) the redirection of flows into the center of the channel and (2) the temporary fining of the streambed in some places due to construction activities. For example, at one of the cross sections, prior to construction, the streambed was composed of 80% gravel compared to 13% gravel immediately after construction. Two postconstruction storm events flushed much of the sand-sized material out of the cross section, and by November 2007, the streambed again was composed of 80% gravel (Figure 5). Similar trends occurred for all cross sections. Because 2007 was a relatively dry year, plants had to be watered periodically during the first growing season. The survival rate of the purchased plants is shown to decrease to about 75% through July 2007, to 55% through November 2008, and to 45% through February 2010 (Figure 6). Survival rates may, in fact, be greater by about 40% representing those plants that could not be located.

3.2. Restoration Objectives 2 and 3: Iterative Modeling to Quantify Sediment Delivery From Stream Banks and Potential Reductions using Different Mitigation Strategies

To address restoration objectives that require a determination of gross amounts of sediment delivery from stream banks, simulations must be performed over a range of hydraulic and geotechnical conditions representing series of flow hydrographs. Quantifying stream bank erosion is not a matter of developing a simple relation (i.e., power function) between flow and sediment delivery. Moderate flows may undercut the bank toe but still not cause mass failure unless bank saturation causes sufficient loss of matric suction and generation of pore water pressure to weaken the bank mass to result in failure. High flows that are often effective at eroding

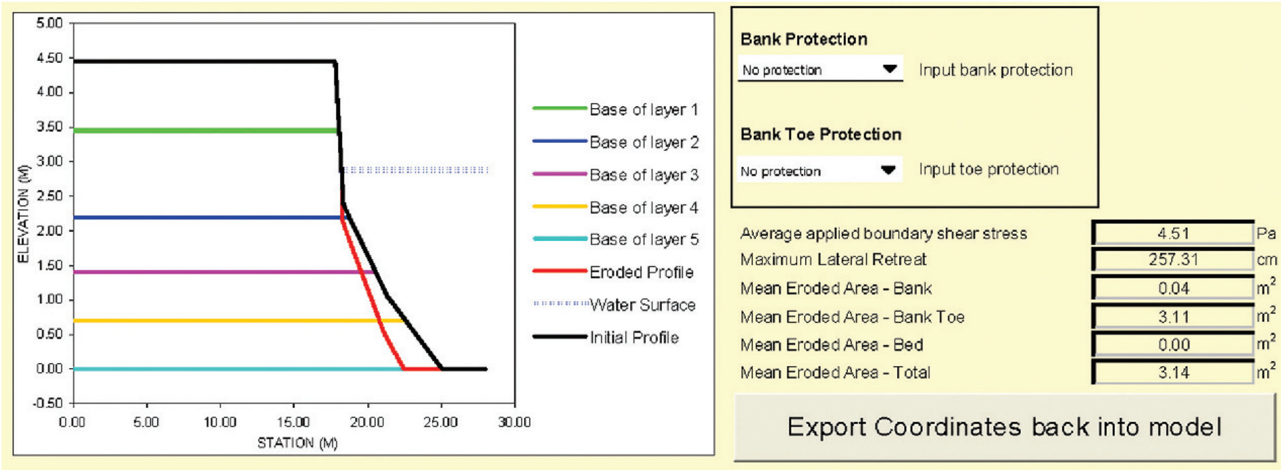

Plate 2. Example results from toe erosion submodel of first flow event and resulting hydraulic erosion.

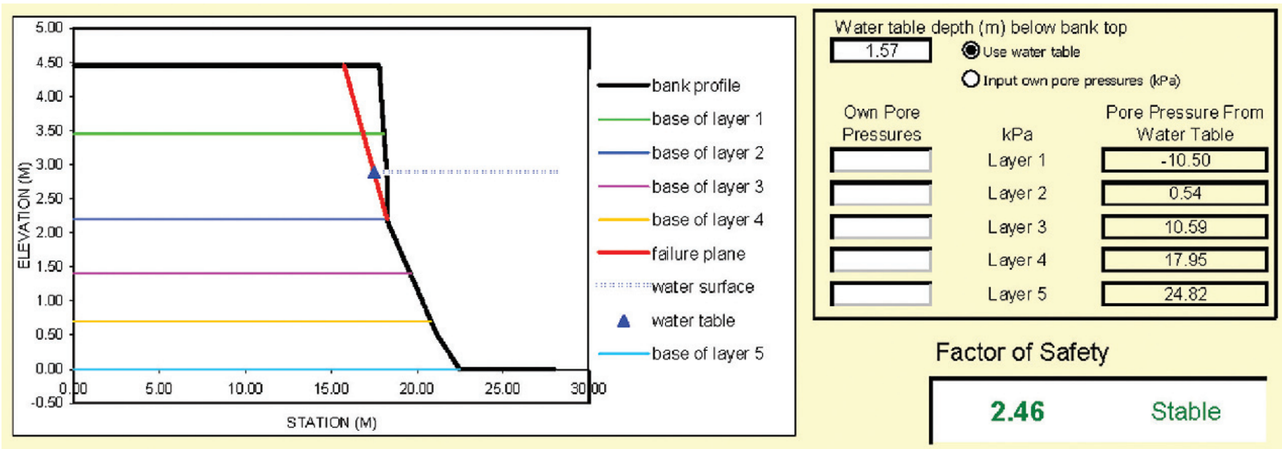

Plate 3. Example results from the bank stability submodel following the first flow event. This simulation shows a stable bank.

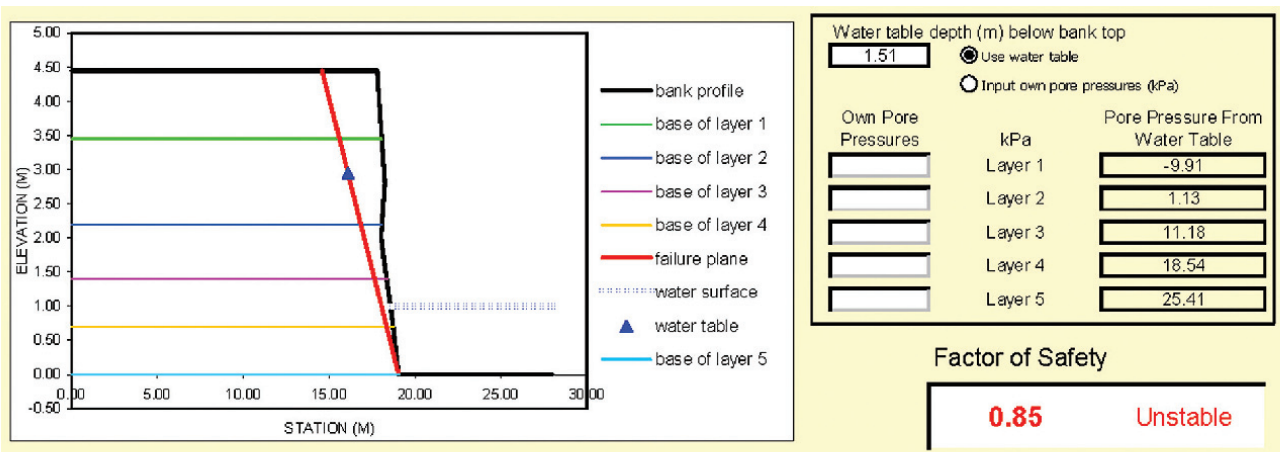

Plate 4. Example results from the bank stability submodel showing an unstable bank under drawdown conditions. In this case, the bank geometry exported to simulate the next flow event is represented by the failure plane (in red) and the original bank toe.

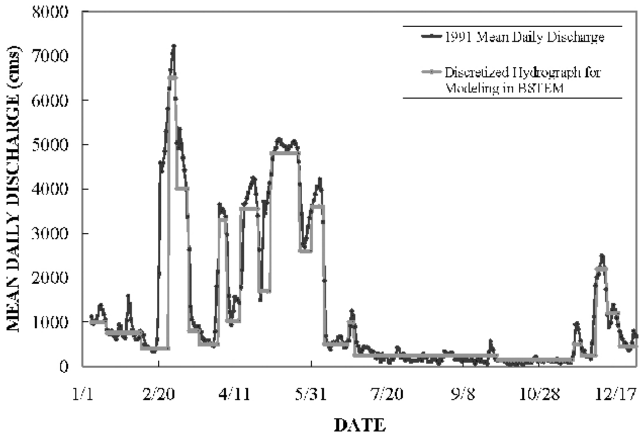

Figure 7. Example of discretized hydrograph for the Lower Tombigbee River, Alabama (below Coffeeville Dam) for the 90th percentile flow year (1991). The numbers 1–6 indicate the storms with discharges that exceeded the critical shear stress of the toe material and were modeled iteratively at this site. From the work of *Bankhead et al.* [2008].

the bank toe may prevent, or at least delay, mass failure because of the confining force provided by the flow that buttresses the bank. In fact, bank failures commonly occur on the recessional limb of storm hydrographs when the banks have lost geotechnical strength due to the effects of pore water pressure and the confining force provided from streamflow. It is for these reasons that analysis, therefore, must be conducted iteratively for a series of hydrographs so that variations in pore water pressure and surface water stage can be accounted for.

Depending on the project needs, iterative model runs were made to represent stream bank dynamics for a range of flow years: a 90th or 99th percentile flow year is used to represent a very wet year and, therefore, potential worst-case conditions for erosion, bank failures, and suspended sediment loadings. A range of flow years was also modeled in two of the case studies presented herein so that the suspended sediment loadings from an average annual year could be calculated. In addition, BSTEM was run with different mitigation strategies to see how, for example, the effect of placing rock at the bank toe or growing different types of vegetation on the banks might affect bank stability and sediment delivery to the channel. The following sections outline the general methods and results of three studies carried out using iterative runs of BSTEM. The flow years and mitigation strategies modeled varied according to the river system being studied and the project objectives.

3.2.1. Lower Tombigbee River, Alabama. Stream bank erosion is prevalent along the Lower Tombigbee River, Alabama. Aerial reconnaissance using GPS-linked video indicated that more than 50% of all banks along the study reach between river kilometer (RKM) 115 and 417 have experienced recent bank failures [*Bankhead et al.*, 2008]. Associated with this erosion is the loss of land and property. Taking the average widening rate of 1.2 m yr^{-1} over the 29 year period of air photo analysis and multiplying by the length of the study reach (301 km) provided an estimate of the total land loss over the period. This was equivalent to about 1040 ha. Given this considerable amount of land loss from bank instabilities, potential strategies to reduce the magnitude and

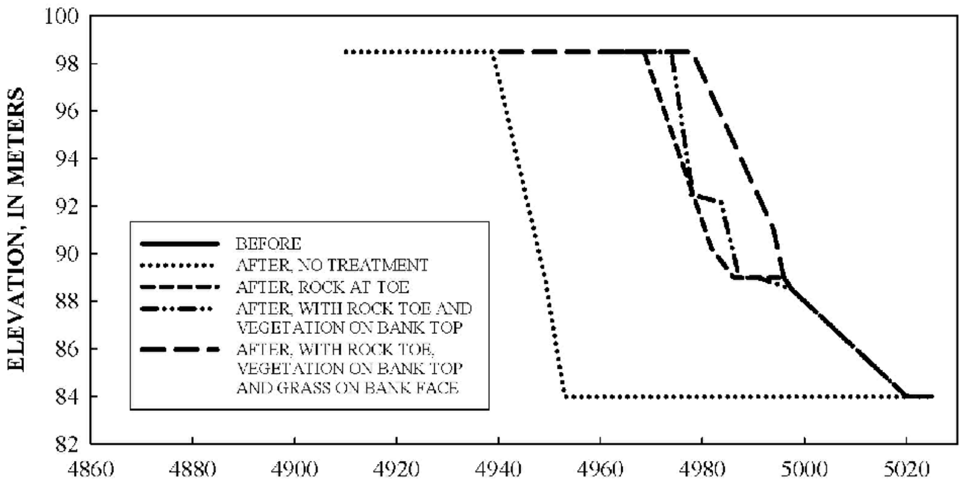

Figure 8. Summary of iterative modeling results for alternative mitigation strategies showing the volume of failures for each bank condition. Modified from the work of *Bankhead et al.* [2008].

Table 8. General Site Characteristics for the Modeled Stream Banks

Stream	River Kilometer (RKM)	Bank Height (m)	Special Characteristics
Blackwood Creek	1.94	3.0	no top bank vegetation
	2.39	2.4	Lemmon's willow (moderate)
Upper Truckee River	4.51	2.6	meadow vegetation
	8.45	1.9	mixed meadow and woody vegetation
	13.1	2.7	golf course with lodgepole pine
Ward Creek	2.48	14.9	14.9 m steep, terrace slope adjacent to channel; coarse material at toe; mature conifers
	3.60	1.3	meadow vegetation

frequency of bank failures along the study reach were investigated.

As an example, a series of alternative strategies to reduce the magnitude and frequency of bank failures was simulated for the site at RKM 184.5. Given that the BSTEM model simulates failures in two dimensions (height and width), a reach length of 100 m was assumed to provide results in m^3. Simulations were conducted in such a way as to be able to quantify the reduction in the frequency of failures and the volume of material delivered to the channel by bank failures. This was accomplished by running the toe erosion and bank stability submodels iteratively for a high-flow year (1991, 90th percentile flow year) to represent worst-case flow conditions. The 1991 flow year contained six major flow events. Mean daily discharge data were used, converted to daily stage, and used in conjunction with a surveyed bed slope of 0.000088 m m^{-1} for the toe erosion submodel. Geotechnical data were collected in situ. To test for the effectiveness of reducing stream bank loadings, iterative modeling was carried out for (1) existing conditions, no mitigation; (2) rock placement along the bank toe; (3) rock placement at the bank toe and 5 year old woody vegetation on the bank top; and (4) rock placement at the bank toe, 5 year old woody vegetation on the bank top, grading the bank to a 45° (1:1) slope, and 5 year old woody vegetation on the regraded slope.

The selected annual hydrograph(s) for the river were discretized into a series of steady state rectangular-shaped discharge events (Figure 7), where the peak of each rectangular hydrograph was set to 90% of the actual hydrograph peak for each storm event. The reason for this reduction in flow peak for each part of the discretized hydrograph was so that the discretized peaks represented the average value occurring over that time period.

Discharge values for each flow event were converted to a series of flow depths, based on a stage-discharge relation developed for the closest U.S. Geological Survey (USGS) gauge to each site. As water table information was unavailable, it was assumed that water table height equaled the flow height at the peak of each hydrograph. For the critical, drawdown condition, the water table was simulated to be equal to the peak flow elevation. For each flow event, the discretized hydrograph was input into BSTEM as a flow depth and peak duration using the following approach:

1. The effects of the first flow event were simulated using the toe erosion submodel to determine the amount (if any) of hydraulic erosion and the change in geometry in the bank toe region (Plate 2).
2. The new geometry was exported into the bank stability submodel to test for the relative stability of the bank. (1) If the F_s was greater than 1.0, geometry was not updated, and the next flow event was simulated (Plate 3). (2) If F_s was less than 1.0, failure was simulated, and the resulting failure plane became the geometry of the bank for simulation of toe erosion for the next flow event in the series. (3) If the next flow event had a stream stage elevation lower than the previous one, the bank stability submodel was run again using the new lower stream stage elevation and higher groundwater table elevation to test for stability under drawdown conditions. If F_s was less than 1.0, failure was simulated, and the new bank geometry was exported into the toe erosion submodel for the next flow event (Plate 4).
3. The next flow event in the series was simulated.

For each set of conditions, the total number of bank failures and the volume associated with each failure was summed and then compared to the other alternatives to quantify the effectiveness of each treatment. For the initial case with existing bank conditions, 11 failures were simulated, resulting in about 55,000 m^3 of eroded bank sediment. Although the number of bank failures was only reduced by 1 (to 10) for the case with toe protection, the amount of lateral retreat and volume of failed material was drastically reduced (by about 500%) to about 9500 m^3. This was because the toe protection did not allow the bank to be undercut at its base, thereby reducing the size of subsequent failures. The addition of bank top vegetation provided additional cohesive strength to the top 1.0 m of the bank and resulted in a further reduction of failure frequency (to 8) and failure volume (8500 m^3). This effect would probably be more pronounced if older specimens were simulated because of greater root density and diameters. Alternative 4, which included rock at the bank toe, grading the bank slope to 1:1 and placing woody vegetation on the bank top and face, greatly reduced failure frequency (to 3) and showed the smallest failure volume of all cases (about 3200 m^3). Results from each of the alternative strategies are shown in graphic form in Figure 8.

Application of these treatments represents a broad range of options and costs. It is important to recognize, however, that both the absolute frequency and volume of failures likely represents an overestimate of what actually took place during 1991. This is because once failure is simulated, the model does not account for the fate of this material, which may be deposited at the bank toe, providing a buttressing (stabilizing) effect and serving to build up the bank toe region. What is relevant are the relative differences between the exiting case (no mitigation) and the various alternatives.

3.2.2. Lake Tahoe Basin, California and Nevada. In this case study, the project objectives were to determine the type of load reductions that could be realized by applying select mitigation measures to stream banks of several streams in the Lake Tahoe Basin, California and Nevada. Cooperators were interested in reducing the delivery of fine-grained sediment from the three main contributors (Upper Truckee River and Blackwood and Ward Creeks) to Lake Tahoe due to decreasing

Table 9. Iterative Modeling Results for the Upper Truckee River (RKM 13.1) for Existing Conditions With Toe Protection[a]

				SW=GW			Drawdown						
Event	Shear Stress (Pa)	Toe Erosion	Volume (m^3)	FS	Failure	Volume (m^3)	FS	Failure	Volume (m^3)	Shear Emergence (m)	Failure Angle (deg)	Total Volume (m^3)	Total Fines (m^3)
Existing Conditions (Assuming 100 m Reach)													
1	6.57	yes	0.70	1.22	no	0.00	1.21	no	0.00	1912.03	40	0.70	0.13
2	6.32	yes	8.50	0.95	yes	362			0.00	1911.88	40	371	67.4
3	8.12	yes	1.40	1.56	no	0.00	1.49	no	0.00	1911.91	34	1.40	0.25
4	5.34	yes	0.30	1.47	no	0.00	1.45	no	0.00	1911.88	34	0.30	0.05
5	2.53	yes	0.20	1.29	no	0.00		no	0.00	1911.88	34	0.20	0.04
6	7.08	yes	3.50	0.99	yes	194	1.37	no	0.00	1911.88	44/32	198	35.9
7	6.55	yes	0.50	1.48	no	0.00			0.00	1911.98	32	0.50	0.09
8a	7.89	yes	64.0	0.91	yes	194			0.00	1911.88	46	258	47.0
8b	7.89	yes	8.70	0.97	yes	185	1.29	no	0.00	1911.88	44.5/32	194	35.3
9	6.46	yes	1.10	1.41	no	0.00	1.35	no	0.00	1911.94	34.5	1.00	0.20
10	3.04	no	0.00	1.51	no	0.00	1.49	no	0.00	1911.94	34.5	0.00	0.00
11	3.13	no	0.00	1.50	no	0.00	1.47	no	0.00	1911.94	34.5	0.00	0.00
12	5.18	yes	0.00	1.35	no	0.00	1.28	no	0.00	1911.91	34.5	0.00	0.00
1/1/1997	13.8	yes	1.60	1.03	no	0.00	0.35	yes	262	1911.88	34.5	264	48.0
Totals		12	90.5		3	935		1	262			1288	234
Toe Protection (Assuming 100 m Reach)													
1	6.57	no	0.00	1.41	no	0.00	1.40	no	0.00	1912.10	40	0.00	0.00
2	6.32	no	0.00	1.44	no	0.00			0.00	1912.10	40	0.00	0.00
3	8.12	no	0.00	1.31	no	0.00	1.25	no	0.00	1912.10	40	0.00	0.00
4	5.34	no	0.00	1.36	no	0.00	1.34	no	0.00	1912.10	40	0.00	0.00
5	2.53	no	0.00	1.38	no	0.00			0.00	1912.10	40	0.00	0.00
6	7.08	no	0.00	1.27	no	0.00	1.19	no	0.00	1912.10	40	0.00	0.00
7	6.55	no	0.00	1.33	no	0.00			0.00	1912.10	40	0.00	0.00
8	7.89	no	0.00	1.26	no	0.00	1.13	no	0.00	1912.10	40	0.00	0.00
9	6.46	no	0.00	1.34	no	0.00	1.30	no	0.00	1912.10	40	0.00	0.00
10	3.04	no	0.00	1.45	no	0.00			0.00	1912.10	40	0.00	0.00
11	3.13	no	0.00	1.44	no	0.00	1.43	no	0.00	1912.10	40	0.00	0.00
12	5.18	no	0.00	1.36	no	0.00	1.32	no	0.00	1912.10	40	0.00	0.00
1/1/1997	13.8	yes	0.10	1.19	no	0.00	0.28	yes	137	1912.10	40	137	25.0
Totals			0.1		0	0.0		1	137			137	25.0

[a]Abbreviations are as follows: FS, factor of safety; SW=GW, surface water level equals groundwater level.

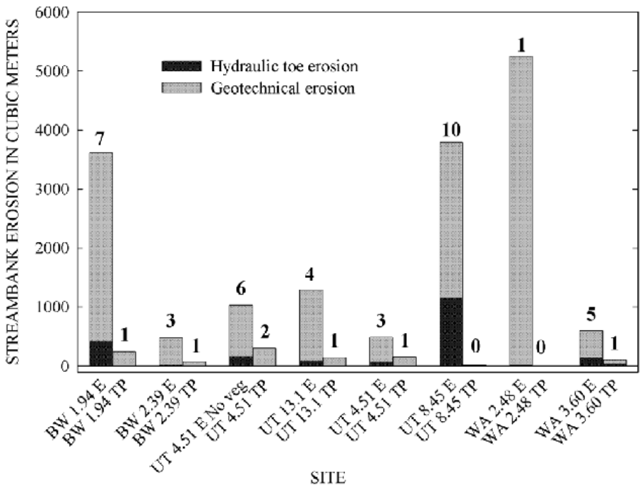

Figure 9. Volume of stream bank erosion under existing (E) conditions and with toe protection (TP) for sites on Blackwood Creek (BW), Upper Truckee River (UT), and Ward Creek (WA). Note the large reduction in total eroded volume for each site by virtually eliminating toe erosion. Bold numbers refer to the number of failure episodes during the 99th percentile flow year. From the work of *Simon et al.* [2009].

lake clarity. A previous study had identified that about 25% of the fine-grained sediment entering the lake emanated from eroding stream banks, with the Upper Truckee River being the largest contributor [*Simon*, 2008]. More than 50% of the suspended-sediment load from the Upper Truckee River and Blackwood Creek is derived from stream bank erosion. A 99th percentile flow year including 12 flow events and a sustained snowmelt period was selected to simulate stream bank erosion with and without various mitigation strategies. In addition, a rain on snow event that occurred on 1 January 1997 and was estimated at about a 50 year recurrence interval was added to the end of the hydrograph. Geotechnical characteristics of the banks and riparian vegetation were determined in situ as part of previous studies [*Simon et al.*, 2003, 2006]. Root reinforcement calculations were made within BSTEM by the RipRoot submodel according to the characteristics shown in Table 8.

Using BSTEM iteratively and under existing conditions at RKM 13.1, a total of 1288 m^3 of material was predicted to be eroded during 12 periods of hydraulic erosion and four mass failure episodes [*Simon et al.*, 2009] (Table 9). Toe erosion represented just 7% of the total bank erosion in the reach. The addition of toe protection virtually eliminated bank steepening by hydraulic erosion at the bank toe, and total bank erosion was reduced by about 89% to 137 m^3 over the same period. Similar results were obtained for all other paired simulations at additional sites (Figure 9) with an average load reduction of 86.8% using toe protection. This result highlights the important relation between hydraulic erosion at the toe that steepens bank slopes and subsequent bank instability. Under existing conditions, toe erosion accounted for an average of 13.6% of the total stream bank erosion, yet control of that process resulted in a total sediment load reduction from bank erosion of almost 87%.

To estimate the total load reduction that could be anticipated for the entire length of each stream, modeled results were combined with observations of the longitudinal extent of recent bank failures along the main stem lengths of each stream. Rapid geomorphic assessments (RGAs) that use diagnostic characteristics of channel form to infer dominant active processes were conducted along each stream as part of earlier research [*Simon et al.*, 2003]. The longitudinal fraction of banks experiencing recent failures was noted for each bank in a reach (6–20 channel widths in length) and expressed as one of five percentage ranges (0%–10%, 11%–25%, 26%–50%, 51%–75%, 76%–100%) (Table 1). The midpoint of the range for each bank (left and right) was used to determine a local mean failure extent. This was then classified as low, moderate, or high in order to apply different unit loads along each stream. Unit loads associated with each class were selected by comparing bank-derived sediment volumes estimated by the numerical simulations with the results of RGAs. For reaches classified as low, a load an order of magnitude lower than the moderate value was used. Unit loads were multiplied by a weighting factor representing the total length of banks (left and right) that had recently failed in a reach to obtain total stream bank-derived sediment loads for the stream. The average extent of bank failures (in percent) was then broken into low, medium, and high groupings to apply different unit loading rates along each stream according to the following procedure. Sediment loads were calculated for each reach by applying the appropriate total loading rate (high or moderate) to those classed as high or moderate. For reaches classified as low, a value an order of magnitude lower than the moderate rate was used. Fine-grained loads for each reach were calculated using the measured percentage of fines (<0.063 mm) for the site. Table 10 shows an example for Blackwood Creek.

To address the cost of potential management scenarios for fine-grained load reduction by toe protection, three options were considered, which included treating all reaches (All), treating only those reaches eroding at high rates (H), and treating only those reaches eroding at high and moderate rates (H+M) (Table 11). A cost for rock placement of \$984 m^{-1} was used as the cost basis (obtained from local sources) that was then multiplied by the length of reach represented by each treatment option. The 86.8% average load reduction obtained for all paired simulations was used to determine the

Table 10. Example Calculation of Total Stream Bank Loads From Blackwood Creek[a]

Distance (km)	Extent of Failures (%) Left	Right	Mean	Reach Length (km) 1	Reach Failing (%) 2	Weighting Factor (1)*(2)/100	Total Volume (m^3)	Fraction <0.063 mm (%)	Fines Volume (m^3)
8.29	0–10	0–10	5.0						
8.19	0–10	26–50	21.5[b]	0.10	13.25	0.0133	62.5[b]	5.8	3.6[b]
7.69	11–25	11–25	18.0[c]	0.50	19.75	0.0987	46.6[c]	0.00	0.00[c]
7.18	11–25	11–25	18.0[c]	0.51	18	0.0918	43.3[c]	26.0	11.3[c]
7.17	11–25	76–100	53.0[d]	0.01	35.5	0.0035	128[d]	26.0	33.4[d]
6.84	0–10	11–25	11.5[c]	0.33	32.25	0.1064	50.2[c]	26.6	13.4[c]
6.51	0–10	51–75	34.0[b]	0.33	22.75	0.0751	354[b]	22.1	78.3[b]
6.03	0–10	26–50	21.5[b]	0.48	27.75	0.1332	629[b]	20.0	125.7[b]
5.55	0–10	26–50	21.5[b]	0.48	21.5	0.1032	487[b]	7.9	38.5[b]
5.08	0–10	51–75	34.0[b]	0.47	27.75	0.1304	616[b]	23.5	144.7[b]
4.15	26–50	11–25	25.5[b]	0.93	29.75	0.2767	1306[b]	3.6	47.0[b]
3.95	0–10	76–100	46.5[d]	0.20	36	0.0720	2604[d]	21.4	557.3[d]
2.80	51–75	0–10	34.0[b]	1.15	40.25	0.4629	2185[b]	12.3	268.7[b]
1.97	26–50	11–25	25.5[b]	0.83	29.75	0.2469	1165[b]	24.8	289[b]
1.77	11–25	51–75	40.5[d]	0.20	33	0.0660	2387[d]	16.6	396.3[d]
0.32	51–75	0–10	34.0[b]	1.45	37.25	0.5401	2549[b]	16.3	415.6[b]
0.00	26–50	26–50	38.0[b]	0.32	36	0.1152	544[b]	16.3	88.6[b]

[a]Results of RGAs (columns 2 to 3) permitted a mean percentage of each reach experiencing bank failures to be estimated. The mean value for the percent failing of consecutive reaches was multiplied by the reach length to calculate the weighting factor for each reach. Fine-grained loads were determined by multiplying the fraction of fines in each reach by the estimated total load.

[b]Moderate (4720 m^3 km^{-1}) stream bank–derived unit loads [see *Simon et al.*, 2009].

[c]Low (472 m^3 km^{-1}) stream bank–derived unit loads [see *Simon et al.*, 2009].

[d]High (36,170 m^3 km^{-1}) stream bank–derived unit loads [see *Simon et al.*, 2009].

reduced load for each protected reach. These reduced loads were then summed for each applicable reach to obtain the load (in t) for the entire stream under the three treatment alternatives (All, H, and H+M). These load values were then compared to the existing load (no treatment) to determine the "potential" load reduction for each of the three streams. These ranged from ranged from 33% to 87% depending on the treatment option (length treated). The unit cost (in \$ t^{-1}) of performing this type of rehabilitation similarly varied from \$267 t^{-1} to almost \$2500 t^{-1} (Table 11).

Additional simulations were carried out to quantify the effects of the addition of top bank vegetation and, in one case, a reduction in bed slope. Load reductions of about 53% were simulated for the case on the Upper Truckee River where root reinforcement was provided to the top 1.0 m of the bank. For locations with higher banks, load reductions

Table 11. Loads and Costs for Performing Bank Toe Protection Assuming a Unit Cost of \$984 m^{-1} for Placement of Stone at the Bank Toe[a]

Stream	Loads (t) Existing	Toe Protection All	H+M	H	Total Cost (\$) Toe Protection All	H+M	H	Unit Cost (\$ t^{-1} of Load Reduction) All	H+M	H
Blackwood Creek	4432	585	623	2920	8,159,449	6,840,551	403,543	2,121	1,796	267
Load reduction (%)		86.8	85.9	34.1						
Upper Truckee River	5691	751	914	3789	20,911,417	10,735,138	2,601,378	4,233	2,247	1,368
Load reduction (%)		86.8	83.9	33.4						
Ward Creek	2956	390	451	910	6,358,661	3,120,669	1,731,594	2,478	1,246	846
Load reduction (%)		86.8	84.7	69.2						
Totals	13,079				35,429,527	20,696,358	4,736,515			

[a]H+M refers to reaches designated as high and moderate.

would probably not be as significant because the limited extent of rooting depths would provide a smaller increase in overall bank strength. Load reductions from the flattening of bed slope (by the addition of meanders) and the consequent decrease in boundary shear stresses were 54% for the case of the Upper Truckee River and 42% for Blackwood Creek.

3.2.3. Big Sioux River, South Dakota. Excessive sediment transport in the Big Sioux River, South Dakota, led action agencies to consider erosion-control strategies in this agricultural basin. Before planning and design of mitigation measures could be conducted, however, it was decided to determine the contributions from stream bank and upland sources so that erosion-control measures could be focused on specific areas of high unit loadings. The objectives of this study, therefore, were to determine (1) average, annual rates of stream bank erosion; (2) the contribution of stream bank erosion to total erosion from other sources; and (3) the effects of possible bank mitigation strategies where necessary.

To obtain average, annual stream bank loads, BSTEM was run iteratively for a range of flow years representing the 10th (dry flow year) through the 90th (very wet) percentile flow years. The volumes of sediment eroded during each percentile flow year modeled were then weighted according to their likely frequency of occurrence to calculate suspended sediment load on an average, annual basis. Results were extrapolated spatially for the entire study reach and then compared to suspended-sediment loads calculated from available data at a USGS gauge along the study reach.

Bank stability and toe erosion analyses were carried out using BSTEM, at five study sites along a 300 km reach of the Big Sioux River, South Dakota, for a range of percentile flow years (90th, 75th, 50th, 25th, and 10th) [*Bankhead and Simon*, 2009]. An example of the flow years that were discretized are shown for USGS gauge 06480000 in Figure 10. Model results showed that eroded volumes of sediment emanating from stream banks decreased nonlinearly from the 90th percentile flow year to the 10th percentile flow year. Predicted volumes of sediment eroded at each site ranged from 169 to 1359 m^3 of sediment per 100 m reach during the 90th percentile year, under existing conditions where the banks have a cover of native grasses (Table 12). These volumes of eroded sediment were predicted to fall to 0 to 21 m^3 per 100 m reach during the modeled 10th percentile flow year, again, assuming a cover of native grasses.

Table 12. Unit Load Values per 100 m of Channel for the Control Case of Existing Geometry With Top Bank Grasses

	Percentile of Flow Magnitude[a]				
Site	90	75	50	25	10
Castlewood	473	42	28	2	10
Estelline	169	98	40	17	12
Brookings	972	200	125	13	10
Egan	1359	218	190	32	21
Renner	680	78	25	29	0

[a]Volume eroded in m^3 $(100\ m)^{-1}$.

Although simulations were conducted for the range of flow years, bank failures were generally predicted only during the 90th percentile flow year at each site. Loads simulated during lower-percentile flow years indicated that hydraulic scour at the bank toe was the predominant erosion process, rather than mass wasting of the banks by geotechnical failure. It followed, therefore, that the addition of toe protection (up to 1 m high) to banks with existing native grass cover greatly reduced the volume of bank material eroded at each site. Model runs indicated that even when the contribution to total erosion from toe scour was not that great (e.g., only 16% to

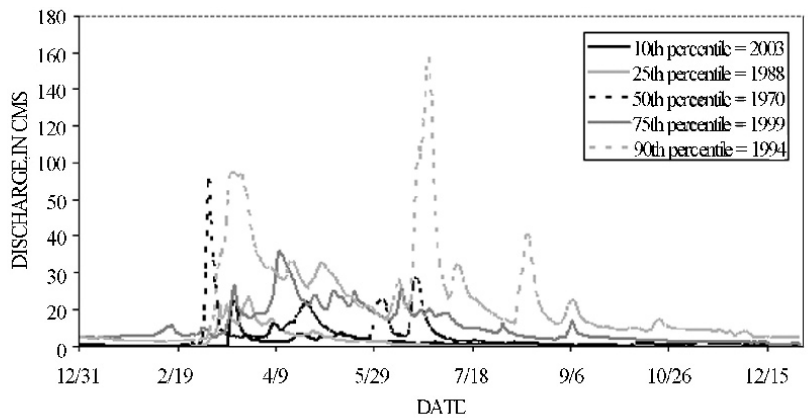

Figure 10. Flow years used for iterative modeling of selected sites on the Big Sioux River, South Dakota. Data are from USGS gauge 06480000. From the work of *Bankhead and Simon* [2009].

Table 13. Example Results of Weighting Values to Produce Average, Annual Stream Bank Loadings Expressed as a Unit Volume and a Unit Mass[a]

	Percentile of Flow Magnitude[b]					Average Annual Loadings		
Site	90	75	50	25	10	Cubic Meters per 100 m	Cubic Meters per Kilometer	Tons per Kilometer
Castlewood	47.3	10.5	14.0	1.5	9.0	82.3	823	14.3
Estelline	16.9	24.5	20.0	12.8	10.8	85.0	850	15.3
Brookings	97.2	50.0	62.5	9.8	9.0	228	2285	40.9
Egan	136	54.4	95.0	24.0	18.9	328	3282	58.1
Renner	68.0	19.5	12.5	21.8	0.0	122	1218	20.6

[a]Weighting values are from Table 12.
[b]Volume eroded in m^3 $(100\ m)^{-1}$.

50% of total erosion came from toe scour during years where bank failures did occur), if the toe scour was prevented, the overall volume of eroded bank material was reduced by 87%–100%.

Average, annual volumes of stream bank sediment emanating from each of the modeled reaches were calculated using weighted values for each percentile flow year (Table 13). These were then converted to $m^3\ km^{-1}$ by multiplying by 10 and then to $t\ km^{-1}$ by multiplying by the bulk unit weight of the material. Average bulk unit weights of the bank material for each site ranged from 16.9 to 18.0 kN m^{-3} [*Bankhead and Simon*, 2009].

Contributions of sediment from stream bank erosion along the study reach of the Big Sioux River were in the range of 10%–25% of the total suspended-sediment load. Average, annual contributions of sediment from stream bank erosion for the entire study reach (6340 t) were shown to be about 15%. During a particularly wet, high-flow year as occurred in 1994, stream bank contributions were consequently greater (27,000 t), comprising 25% of the total suspended-sediment

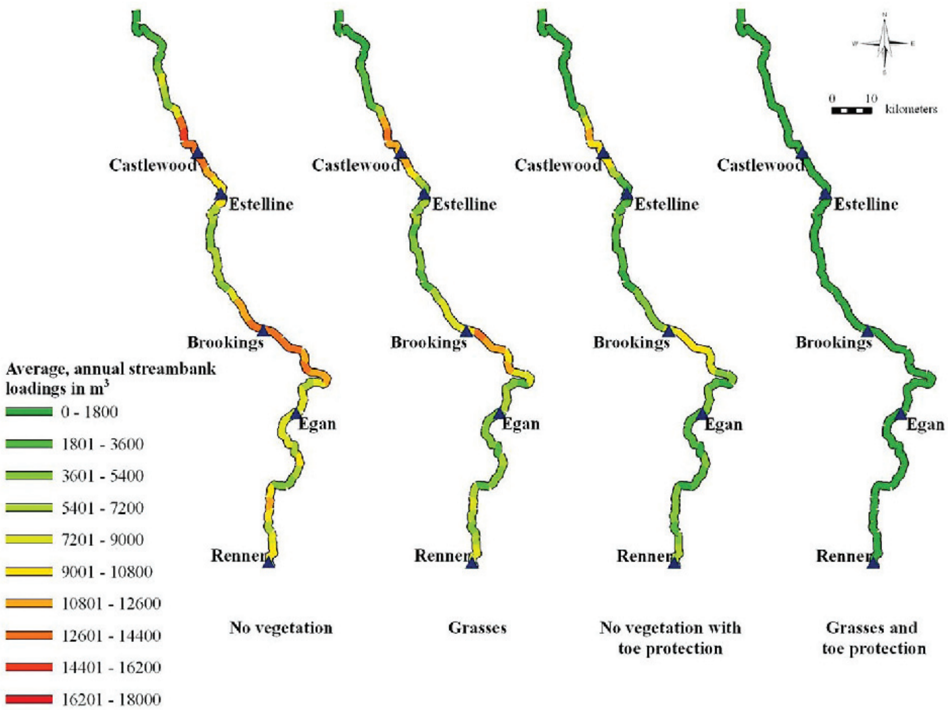

Plate 5. Illustration of spatial distribution of average, annual stream bank loads (m^3) for a range of mitigation strategies and bank conditions along the Big Sioux River, South Dakota. From the work of *Bankhead and Simon* [2009].

load over the 300 km study reach. The data further indicated that stream bank contributions were generally greater in the lower half of the study reach.

The iterative modeling results from the five sites needed to be interpolated and extrapolated over the 300 km study reach to determine total loads and potential load reductions for the mitigation strategies tested. As expected, the bare-bank simulations displayed greater average, annual loadings along the entire study reach, with total loads of 503,000 m^3 (8810 t). The effect of top bank grasses (or an assemblage of grasses and young cottonwood trees) resulted in a reduction of average, annual stream bank loads of 28% (to 362,000 m^3 or 6340 t); 20% for the 90th percentile flow. The addition of bank toe protection to the grassed bank resulted in a total reduction in average, annual loads (from the bare-bank case) of 97% (to 15,200 m^3 or 267 t). The important role of toe protection was further apparent by comparing the difference in stream bank loads between the bare-bank case and the mitigation strategy that incorporated toe protection alone. Here, average, annual stream bank loads were reduced 51% from 503,000 m^3 (8810 t) to 243,000 m^3 (4250 t); 84% for the 90th percentile flow.

Results of potential mitigation strategies can also be displayed spatially. Maps, such as those shown in Plate 5, can be used to focus stream restoration practitioners to those reaches that are the most problematic and to identify the magnitude of the potential load reductions that could be expected for a given reach and mitigation strategy. For example, in some of the yellow reaches in the map with no vegetation or mitigation, addition of grasses to the bank top may provide enough stability to reduce sediment loading to the required level in that particular reach. In the reaches that are shown in red in the first map, addition of vegetation may not be sufficient, with those reaches also requiring further mitigation, such as rock toe protection, to reduce bank erosion and resulting suspended sediment loadings.

4. CONCLUSIONS

The BSTEM is a simple spreadsheet tool developed to simulate stream bank erosion in a completely mechanistic framework. It has been successfully used in a range of alluvial environments in both static mode to simulate bank stability conditions and design of stream bank stabilization measures and, iteratively, over a series of hydrographs to evaluate surficial, hydraulic erosion, bank failure frequency, and thus, the volume of sediment eroded from a bank over a given period of time. In combination with the submodel RipRoot, the reinforcing effects of riparian vegetation can be quantified and included in analysis of mitigation strategies. In addition, the model has been shown to be very useful in testing the effect of potential mitigation measures that might be used to reduce the frequency of bank instability and decrease sediment loads emanating from stream banks. Finally, the results of iterative BSTEM analysis can be used to spatially extrapolate bank-derived volumes of sediment, from individual sites to entire reaches when used in conjunction with RGAs conducted at regular intervals along the study reach. Results of these case studies have shown that the relative contribution of suspended sediment from stream banks can vary considerably, ranging from as low as 10% in the predominantly low-gradient, agricultural watershed of the Big Sioux River, South Dakota, to more than 50% for two steep, forested watersheds of the Lake Tahoe Basin, California. Modeling of stream bank mitigation strategies has also shown that the addition of toe protection to eroding stream banks can reduce overall volumes of eroded sediment up to 85%–100%, notwithstanding that hydraulic erosion of the toe in this particular case makes up only 15%–20% of total bank erosion. Vegetation provides a stabilizing effect to the modeled stream banks, but sufficient time must be factored into any restoration design involving vegetation as a mitigation measure, to allow sufficient development of root networks.

REFERENCES

Bankhead, N., and A. Simon (2009), Analysis of bank stability and potential load reduction along reaches of the Big Sioux River, South Dakota, *Tech. Rep. 64*, Natl. Sediment. Lab., Argic. Res. Serv., U.S. Dep. of Agric., Oxford, Miss.

Bankhead, N., A. Simon, and D. Klimetz (2008), Analysis of streambank erosion along the Lower Tombigbee River, Alabama, *Tech. Rep. 62*, Natl. Sediment. Lab., Argic. Res. Serv., U.S. Dep. of Agric., Oxford, Miss.

Cancienne, R. M., G. Fox, and A. Simon (2008), Influence of seepage undercutting on the stability of root-reinforced streambanks, *Earth Surf. Processes Landforms*, *33*(8), 1769–1786.

Fredlund, D. G., N. R. Morgenstern, and R. A. Widger (1978), The shear strength of unsaturated soils, *Can. Geotech. J.*, *15*, 313–321.

Gray, D. H. (1974), Reinforcement and stabilization of soil by vegetation, *J. Geotech. Eng. Div. Am. Soc. Civ. Eng.*, *100*(GT6), 695–699.

Hanson, G. J. (1990), Surface erodibility of earthen channels at high stresses: Part II. Developing an in-situ testing device, *Trans. ASAE*, *33*(1), 132–137.

Hanson, G. J. (1991), Development of a Jet index to characterize erosion resistance of soils in earthen spillways, *Trans. ASAE*, *34*(5), 2015–2020.

Hanson, G. J., and A. Simon (2001), Erodibility of cohesive streambeds in the loess area of the midwestern USA, *Hydrol. Processes*, *15*(1), 23–38.

Julien, P. (2002), *River Mechanics*, Cambridge Univ. Press, Cambridge, U. K.

Langendoen, E. J. (2000), CONCEPTS: Conservational channel evolution and pollutant transport system software manual, *Res. Rep. 16*, Natl. Sediment. Lab., Argic. Res. Serv., U.S. Dep. of Agric., Oxford, Miss.

Lohnes, R. A., and R. L. Handy (1968), Slope angles in friable loess, *J. Geol.*, *76*(3), 247–258.

Lutenegger, J. A., and B. R. Hallberg (1981), Borehole shear test in geotechnical investigations, *ASTM Spec. Tech. Publ.*, *740*, 566–578.

Micheli, E. R., and W. Kirchner (2002), Effects of wet meadow riparian vegetation on streambank erosion. 2. Measurements of vegetated bank strength and consequences for failure mechanics, *Earth Surf. Processes Landforms*, *27*, 687–697.

Mickovski, S. B., P. D. Hallet, M. F. Bransby, M. C. R. Davies, R. Sonnenberg, and A. G. Bengough (2009), Mechanical reinforcement of soil by willow roots: Impacts of root properties and root failure mechanism, *Soil Sci. Soc. Am. J.*, *73*, 1276–1285.

Morgenstern, N. R., and V. E. Price (1965), The analysis of the stability of general slip surfaces, *Geotechnique*, *15*(1), 79–93.

Partheniades, E. (1965), Erosion and deposition of cohesive soils, *J. Hydraul. Eng.*, *91*(1), 105–139.

Pollen, N. (2007), Temporal and spatial variability in root reinforcement of streambanks: Accounting for soil shear strength and moisture, *Catena*, *69*, 197–205.

Pollen, N., and A. Simon (2005), Estimating the mechanical effects of riparian vegetation on stream bank stability using a fiber bundle model, *Water Resour. Res.*, *41*, W07025, doi:10.1029/2004WR003801.

Pollen, N., A. Simon, A. J. C. Collision (2004), Advances in assessing the mechanical and hydrologic effects of riparian vegetation on streambank stability, in *Riparian Vegetation and Fluvial Gomorphology*, edited by S. Bennett, and A. Simon, *Water Sci. Appl. Ser.*, vol. 8, pp. 125–139, AGU, Washington, D. C.

Pollen-Bankhead, N., and A. Simon (2009), Enhanced application of root-reinforcement algorithms for bank-stability modeling, *Earth Surf. Processes Landforms*, *34*(4), 471–480.

Selby, M. J. (1982), *Hillslope Materials and Processes*, 264 pp., Oxford Univ. Press, Oxford, U. K.

Shields, A. (1936), Anwendung der Aechlichkeitsmechanik und der Turbulenz Forschung auf die Geschiebebewegung, report, Pruessischen Versuchsanst. für Wasserbau und Schiffbau, Berlin.

Shields, F. D. (2003), Large wood as a restoration tool: I fought the law, and the law won, paper presented at STREAMS Channel Protection and Restoration Conference, Ohio State Univ., Columbus, 6–7 Oct.

Shields, F. D., N. Morin, and C. M. Cooper (2004), Large woody debris structures for sand-bed channels, *J. Hydraul. Eng.*, *130*(3), 208–217.

Simon, A. (2008), Fine-sediment loadings to Lake Tahoe, *J. Am. Water Resour. Assoc.*, *44*(3), 618–639.

Simon, A., and A. J. C. Collison (2002), Quantifying the mechanical and hydrologic effects of riparian vegetation on stream-bank stability, *Earth Surf. Processes Landforms*, *27*(5), 527–546.

Simon, A., and A. Curini (1998), Pore pressure and bank stability: The influence of matric suction, in *Water Resources Engineering '98*, edited by S. R. Abt, J. Young- Pezeshk, and C. C. Watson, pp. 358–363, Am. Soc. of Civ. Eng., Reston, Va.

Simon, A., and M. Rinaldi (2006), Disturbance, stream incision, and channel evolution: The roles of excess transport capacity and boundary materials in controlling channel response, *Geomorphology*, *79*, 361–383.

Simon, A., A. Curini, S. Darby, and E. Langendoen (1999), Streambank mechanics and the role of bank and near-bank processes in incised channels, in *Incised River Channels*, edited by S. Darby and A. Simon, pp. 123–152, John Wiley, New York.

Simon, A., A. Curini, S. E. Darby, and E. J. Langendoen (2000), Bank and near-bank processes in an incised channel, *Geomorphology*, *35*, 193–217.

Simon, A., E. Langendoen, R. Bingner, R. Wells, A. Heins, N. Jokay, and I. Jaramillo (2003), Lake Tahoe basin framework implementation study: Sediment loadings and channel erosion, *Tech. Rep. 39*, 320 pp., Natl. Sediment. Lab., Argic. Res. Serv., U.S. Dep. of Agric., Oxford, Miss.

Simon, A., N. Pollen, and E. Langendoen (2006), Influence of two woody riparian species on critical conditions for streambank stability: Upper Truckee River, California, *J. Am. Water Resour. Assoc.*, *42*(1), 99–113.

Simon, A., D. Derrick, C. V. Alonso, and N. Pollen-Bankhead (2008), Application of a deterministic bank-stability model to design a reach-scale restoration project, in *Proceedings of the World Environmental and Water Resources Congress 2008 Ahupua'a* [CD-ROM], edited by R. W. Babcock Jr. and R. Walton, Am. Soc. of Civ. Eng., Reston, Va.

Simon, A., N. Pollen-Bankhead, V. Mahacek, and E. Langendoen (2009), Quantifying reductions of mass-failure frequency and sediment loadings from streambanks using toe protection and other means: Lake Tahoe, United States, *J. Am. Water Resour. Assoc.*, *45*(1), 170–186.

Simon, A., N. Bankhead, and R. E. Thomas (2010), Iterative bank-stability and toe-erosion modeling for predicting streambank loading rates and potential load reductions, paper presented at Joint Federal Interagency Conference, Subcomm. on Hydrol. and Sediment., Advis. Comm. on Water Info., Las Vegas, Nev., 27 June to 1 July.

Simons, D. B., and F. Senturk (1992), *Sediment Transport Technology, Water and Sediment Dynamics*, 897 pp., Water Resour. Publ., Littleton, Colo.

Thorne, C. R., and N. K. Tovey (1981), Stability of composite river banks, *Earth Surf. Processes Landforms*, *6*, 469–484.

Waldron, L. J. (1977), The shear resistance of root-permeated homogeneous and stratified soil, *J. Soil Sci. Soc. Am.*, *41*, 843–849.

Wu, T. H., W. P. McKinnell, III, and D. N. Swanston (1979), Strength of tree roots and landslides on Prince of Wales Island, Alaska, *Can. Geotech. J.*, *16*, 19–33.

Wyżga, B., P. Oglęcki, A. Radecki-Pawlik, and J. Zawiejska (2011), Diversity of macroinvertebrate communities as a reflection of habitat heterogeneity in a mountain river subjected to variable human impacts, in *Stream Restoration in Dynamic Fluvial Systems: Scientific Approaches, Analyses, and Tools*, *Geophys. Monogr. Ser.*, doi: 10.1029/2010GM00983, this volume.

N. Pollen-Bankhead and A. Simon, National Sedimentation Laboratory, Agricultural Research Service, USDA, PO Box 1157, Oxford, MS, Oxford, MS 38655, USA. (andrew.simon@ars.usda.gov)

R. E. Thomas, School of Earth and Environment, University of Leeds, Leeds LS2 9JT, UK.